RESEARCH ARTICLE

JOURNAL OF
MEDICAL VIROLOGY WILEY

Association between emphysema and other pulmonary computed tomography patterns in COVID-19 pneumonia

Ke Han[1] | Jing Wang[2] | Yulin Zou[2,3] | Yuxin Zhang[2] | Lin Zhou[4] | Yiping Yin[5]

[1]Department of Cardiothoracic Vascular Surgery, Renmin Hospital, Hubei University of Medicine, Shiyan, Hubei, P. R. China

[2]Department of Dermatology, Renmin Hospital, Hubei University of Medicine, Shiyan, Hubei, P. R. China

[3]Department of Dermatology, Jinzhou Medical University Graduate Training Base, Renmin Hospital, Hubei University of Medicine, Shiyan, Hubei, P. R. China

[4]Department of Medical Imaging Center, Renmin Hospital, Hubei University of Medicine, Shiyan, Hubei, P. R. China

[5]Department of Pulmonary & Critical Care Medicine, Renmin Hospital, Hubei University of Medicine, Shiyan, Hubei, P. R. China

Correspondence
Yiping Yin, Department of Pulmonary & Critical Care Medicine, Renmin Hospital, Hubei University of Medicine, Shiyan, Hubei 442000, P. R. China.
Email: 88370618@qq.com

Abstract

To evaluate the chest computed tomography (CT) findings of patients with Corona Virus Disease 2019 (COVID-19) on admission to hospital. And then correlate CT pulmonary infiltrates involvement with the findings of emphysema. We analyzed the different infiltrates of COVID-19 pneumonia using emphysema as the grade of pneumonia. We applied open-source assisted software (3D Slicer) to model the lungs and lesions of 66 patients with COVID-19, which were retrospectively included. we divided the 66 COVID-19 patients into the following two groups: (A) 12 patients with less than 10% emphysema in the low-attenuation area less than −950 Hounsfield units (%LAA-950), (B) 54 patients with greater than or equal to 10% emphysema in %LAA-950. Imaging findings were assessed retrospectively by two authors and then pulmonary infiltrates and emphysema volumes were measured on CT using 3D Slicer software. Differences between pulmonary infiltrates, emphysema, Collapsed, affected of patients with CT findings were assessed by Kruskal–Wallis and Wilcoxon test, respectively. Statistical significance was set at $p < 0.05$. The left lung (A) affected left lung 20.00/affected right lung 18.50, (B) affected left lung 13.00/affected right lung 11.50 was most frequently involved region in COVID-19. In addition, collapsed left lung, (A) collapsed left lung 4.95/collapsed right lung 4.65, (B) collapsed left lung 3.65/collapsed right lung 3.15 was also more severe than the right one. There were significant differences between the Group A and Group B in terms of the percentage of CT involvement in each lung region ($p < 0.05$), except for the inflated affected total lung ($p = 0.152$). The median percentage of collapsed left lung in the Group A was 20.00 (14.00–30.00), right lung was 18.50 (13.00–30.25) and the total was 19.00 (13.00–30.00), while the median percentage of collapsed left lung in the Group B was 13.00 (10.00–14.75), right lung was 11.50 (10.00–15.00) and the total was 12.50 (10.00–15.00). The percentage of affected left lung is an independent predictor of emphysema in COVID-19 patients. We need to focus on the left lung of the patient as it is more affected. The people

1 | INTRODUCTION

In December 2019, a series of patients with unexplained pneumonia was reported in Wuhan, China. There is now clear evidence that the causative agent is a virus from corona virus family. The virus was designated as Corona Virus Disease 2019 (COVID-19) by the World Health Organization (WHO) on 11 February, 2020.[1] As an ongoing global emergency pandemic, the severe acute respiratory syndrome coronavirus 2 is the cause of COVID-19. It primarily affects the respiratory system of patients and also lead to a broad spectrum of clinical manifestations including asymptomatic carriage to respiratory failure and acute respiratory distress syndrome.[2-4] Pneumonia is the most common indication for hospital admission. A significant proportion of the patients require intensive care support.[5] The contact and droplet routes are being advocated as the main modes by leading public health agencies, including WHO. However, these precautionary measures are still not completely. Various empirical conducted in countries, including China, Italy, Singapore, and USA, have elucidated the indoor, as well as outdoor airborne transmission.[6]

It is well known that the gold standard for the diagnosis of COVID-19 infection is considered to be the reverse-transcriptase quantitative real time polymerase chain reaction (RT-qPCR).[7] CT cannot be used alone for the diagnosis of COVID-19 because of its low specificity. In the case of negative RT-qPCR results, CT is useful, but confirmation of the diagnosis of COVID-19 should be achieved by repeat RT-qPCR or serology. However, chest computed tomography (CT) has been reported to be diagnostic in the presence of false negative results of RT-qPCR. It is not only useful in monitoring disease progression, but also in evaluating therapeutic efficacy. Despite the increasing number of patients recovering from COVID-19, there are concerns about the long-term consequences of recovery. There is sufficient evidence that some survivors of COVID-19 may develop long-term respiratory complications.[8-11] Several studies have reported some CT findings in COVID-19 pneumonia, however, estimates of risk factors for severe disease and death are not very robust and research on the relationship between chest CT remains limited. Information from CT scans can allocate limited intensive care resources while assisting emergency physicians in triage of patients.[12,13]

In contrary to the conventional X-ray methods, CT scans of chest can show us more detailed view of blood vessels, lungs and soft tissue.[14] Therefore, artificial intelligence (AI) is needed to learn CT imaging models in depth. Increasingly, AI methods have been developed and then used to sense infected patients.[15-18]

Moreover, to our knowledge, only a few studies have so far analyzed the relationship between pulmonary infiltrates and emphysema in chest CT. Our study aimed to describe the relationship between pulmonary infiltrates and emphysema by means of a CT model in patients of COVID-19.[19-21]

The degree of pulmonary infiltrations and the presence of areas such as emphysema or bullae are usually analyzed visually on CT scans.[22-24] Abnormalities cannot be quantified in numbers or milliliters, making it difficult to compare results objectively. This is particularly critical in the current COVID-19 pandemic situation, where there are many cases of patients with severe pulmonary infiltrates. Lung CT Analyzer (LTCA) enables three-dimensional segmentation of lung CT data and calculation of individual volumes of pulmonary infiltrates and emphysema. In our study, we applied it to model the lungs and lesions of COVID-19 patients for competitive analysis.[25]

2 | MATERIALS AND METHODS

The Institutional Review Board (Ethical Committee, Renmin Hospital, Hubei University of Medicine, Shiyan, China) approved this retrospective observational study and waived the requirement for written informed consent.

2.1 | Study population and data collection

In a large tertiary academic hospital, we conducted this retrospective cohort study. Consecutive patients admitted to our hospital (Renmin Hospital, Hubei University of Medicine, Hubei, China) between February 2 and April 25, 2020 with COVID-19 infection confirmed by real-time reverse transcriptase-polymerase chain reaction, were included in our study. The inclusion criteria were as follows: (a) positive RT-qPCR results on nasal swabs before or after hospitalization, (b) CT examination on admission, (c) hospitalized adult patients (≥18-year-old). Exclusion criteria were: (a) a history of chronic pulmonary disease, (b) poor quality imaging material.

Patients' smoking history, demographics, date of disease onset and chest CT were extracted from electronic patient records. Figure 1 is a flow chart of the study.

2.2 | CT image acquisition and analysis

CT scans of the chest are acquired simultaneously from the base of the lung towards the apex of the lung, in the supine position with full inspiration, using either a 64-slice or a 16-slice scanner
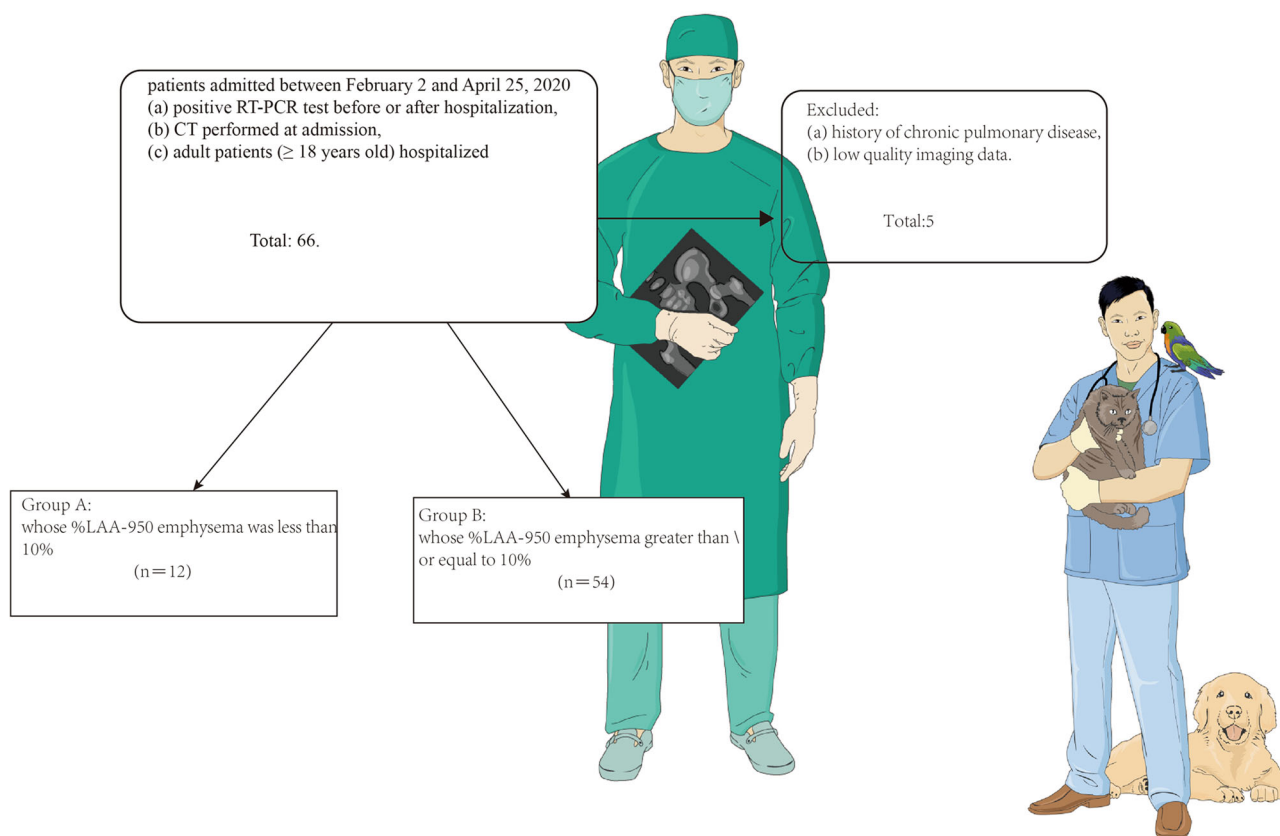
patients admitted between February 2 and April 25, 2020
(a) positive RT-PCR test before or after hospitalization,
(b) CT performed at admission,
(c) adult patients (≥ 18 years old) hospitalized

Total: 66.

Excluded:
(a) history of chronic pulmonary disease,
(b) low quality imaging data.

Total:5

Group A:
whose %LAA-950 emphysema was less than 10%
(n = 12)

Group B:
whose %LAA-950 emphysema greater than \ or equal to 10%
(n = 54)

FIGURE 1 A flow chart of the study

(LightSpeed16). All CT acquisitions were performed without contrast medium. The following parameters were performed: tube voltage, 120 kVp; automatic exposure control of tube current; pitch, 0.8; collimation, 12–40 mm. Images were reconstructed using sharp kernels and standard lung window settings (width, 1200 HU; level, −500 HU) at slice thicknesses 0.9–1.5 mm. The CT images were all taken by the two authors of this paper (Y. L. Z., a resident doctor with 2 years of experience, Y. X. Z., an intern doctor) for acquisition.

We used the open-source 3D Slicer, version 4.13.1 (https://www.slicer.org) to compare damaged lung volume. Lung CT Analyzer (Department of Surgery, Kantonsspital Graubünden [KSGR]) is a 3D Slicer extension for segmentation and spatial reconstruction of infiltrated, emphysematic and collapsed lung areas in CT scans. We performed a volumetric analysis and visualization in 3D Slicer (http://www.slicer.org) via the Lung CT Analyzer project (https://github.com/rbumm/SlicerLungCTAnalyzer/). The software uses definable threshold ranges (remaining airways were further excluded through the Airway Segmentation Module and by imposing a −950 HU baseline minimum. Compromised lung was defined by image density over −800 HU) to identify five regions of interest: "Bulla/emphysema," "Inflated," "Infiltrated," "Collapsed" and "Lung Vessel." Segments are generated using 3DSlicer's segment editor "Threshold" and "Grow from Seeds" function. The volume of each segment is calculated by using 3DSlicer's "Segment statistics" function. The results are then superimposed to the CT 2D views in standard colors: "Bulla" = black, "Inflated" = blue, "Infiltrated" = yellow, "Collapsed" = pink, and "Vessel" = red (Figure 2).

In addition, spatial reconstruction (3D) of the diseased lung segments coudl be performed. The total results of the segmentation included: total lung volume (100%), right lung volume (percentage of total lung volume), left lung volume (percentage of total lung volume), functional right lung volume (inflated, percentage of right lung volume), functional left lung volume (inflated, percentage of left lung volume), functional total lung volume (inflated, percentage of total lung volume), affected right lung volume (infiltrated and collapsed right lung volume, percentage of right lung volume), affected left lung volume (infiltrated and collapsed left lung volume, percentage of left lung volume), affected total lung volume (infiltrated and collapsed total lung volume, percentage of total lung volume).

2.3 | Divide into groups

In Castaldi's study, in %LAA-950 emphysema of less than 10%, the predominant lesion lung class was the mild centrilobular pattern. In %LAA-950 emphysema greater than or equal to 10%, the moderate centrilobular pattern would predominate. In addition, as %LAA-950 emphysema increased, the number of individuals with severe centrilobular, PL, and PB patterns will also increasd.[26] Therefore, we divided the 66 patients with COVID-19 into the following two groups: (A) 12 individuals with %LAA-950 emphysema less than 10% and (B) 54 individuals with %LAA-950 emphysema greater than or
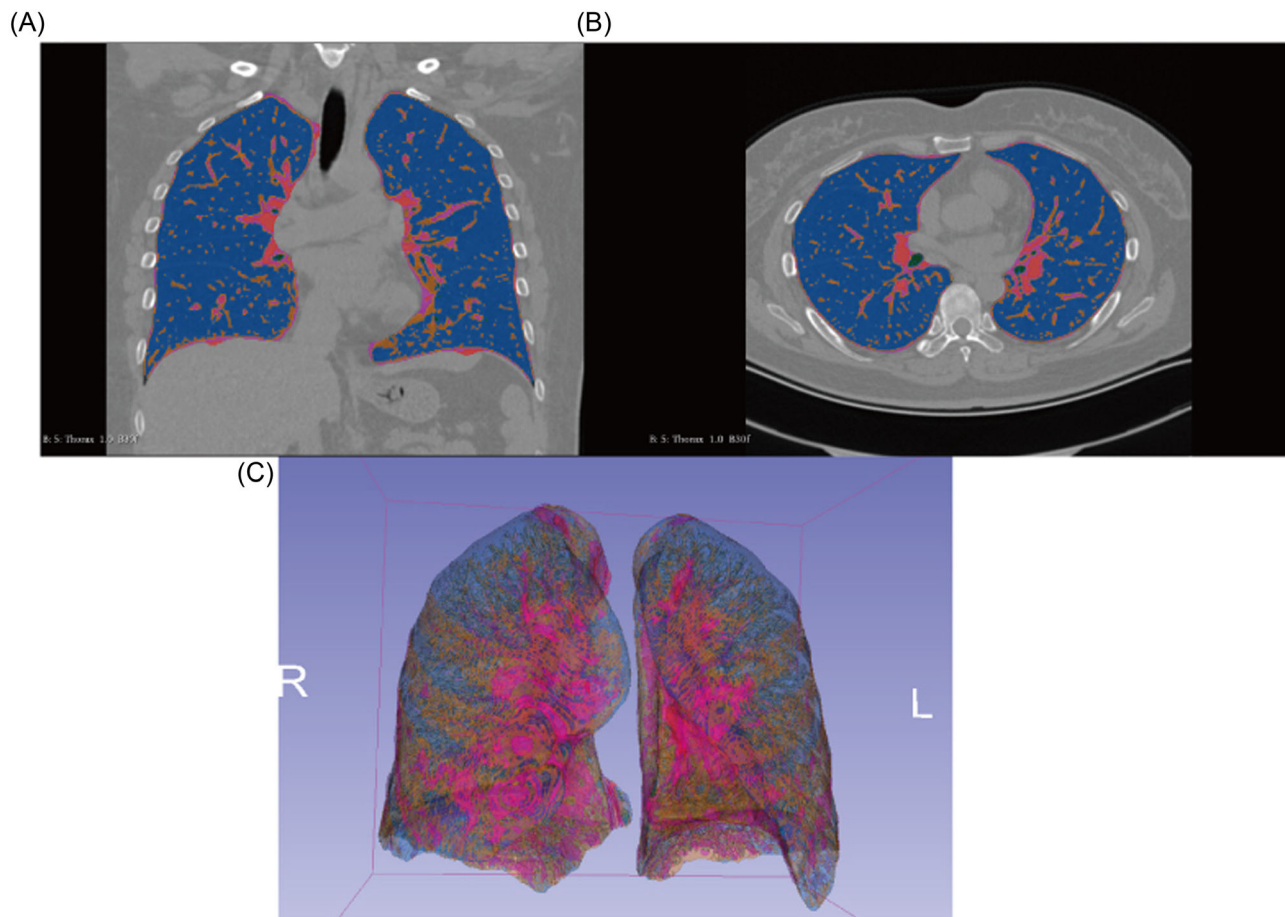
(A) (B)

(C)

FIGURE 2 3D Slicer's segment

equal to 10%. Although previous study have been done on smokers and chronic disease, we still use it in the context of COVID-19 pneumonia as it applies as well.

2.4 | Threshold-based emphysema measures

The threshold-based %LAA-950 measure was calculated for each lung CT scan by sizing the percentage of the entire lung density histogram below the 2950 Hounsfield unit threshold separately.

2.5 | Statistical analysis

Data analysis was carried out using Graphpad Prism (version 9) and SPSS (version 25.0).

We summarized continuous variables using mean ± SD or median and interquartile range (IQR) when appropriate. Categorical variables are presented as n (%). The difference in the demographic data between two clinical groups were compared with Mann–Whitney U-test, χ^2, and Fischer exact tests using permutation method for multiple comparisons. Differences between pulmonary infiltrates, emphysema, Collapsed, affected of patients with CT findings were assessed by Kruskal–Wallis and Wilcoxon test. In all statistical analysis, $p < 0.05$ was considered statistically significant.

Variables with $p < 0.5$ in the univariate analysis were entered into a multivariate logistic regression analysis to identify independent risk factors contributing to %LAA-950 emphysema above 10%.

3 | RESULTS

3.1 | Clinical findings

The clinical data of the 66 COVID-19 patients at the time of admission are shown in Table 1, of whom 54 were in Group A and 12 in Group B. The majority of patients were male (54.5%). The age of the patients ranged from 19 to 85 years, with a mean of 45.70 ± 14.91 years. The most common clinical symptoms were fever (52/66, 78.8%) and cough (23/66, 34.8%). Hypertension was the most common comorbidity of COVID-19 (8/66, 12.1%), followed by diabetes (4/66, 6.1%) and coronary artery disease (4/66, 6.1%). There were significant differences between the two groups in terms of cough ($p = 0.015$), dyspnea ($p = 0.043$), myalgia ($p = 0.012$). Besides, it must be noted that the percentage of fever in Group B is 100%. Table 1 shows the detailed patient characteristics.

TABLE 1 Demographics, comorbidities, symptoms of patients

Variables		All patients (n = 66)	A (n = 54)	B (n = 12)	p Value
Age (years), median (IQR)		45.70 ± 14.91	46.41 ± 14.63	42.50 ± 16.40	0.531[a]
Gender, n (%)	Male	36 (54.5)	30 (55.6)	6 (50)	0.122[b]
	Female	30 (45.5)	24 (44.4)	6 (50)	
Comorbidities n (%)	Diabetes	4 (6.1)	3 (5.6)	1 (8.3)	0.133[b]
	Hypertension	8 (12.1)	6 (11.1)	2 (16.7)	0.284[b]
	Coronary artery disease	4 (6.1)	3 (5.6)	1 (8.3)	0.133[b]
	Chronic lung disease	0 (0)	0 (0)	0 ((0)	-
	Chronic liver disease	0 (0)	0 (0)	0 (0)	-
	Chronic renal failure	0 (0)	0 (0)	0 (0)	-
	Malignancy	0 (0)	0 (0)	0 (0)	-
	Postpartum	2 (3.0)	1 (1.9)	1 (8.3)	1.404[b]
Symptoms	Fever	52 (78.8)	40 (74.1)	12 (100)	3.949[b]
	Cough	23 (34.8)	19 (35.2)	4 (33.3)	0.015[b]
	Dyspnea	15 (22.7)	12 (22.2)	3 (25.0)	0.043[b]
	Myalgia	5 (7.6)	4 (7.4)	1 (8.3)	0.012[b]

Abbreviation: IQR, interquartile range.

[a]Fischer's exact test.

[b]χ^2 test.

3.2 | Imaging findings

Patients with COVID-19 were divided into two groups according to whether their %LAA-950 emphysema was greater than 10%. In Group A, %LAA-950 emphysema was less than 10% and in Group B, %LAA-950 emphysema was greater than or equal to 10%. We analyzed the CT scans of patients in both groups. Segments were created based on their Hounsfield units, using a predefined threshold range.

Overall, the left lung (Group A: left lung 20.00%/right lung 18.50%, Group B: left lung 13.00%/right lung 11.50%) was the region of the lung most frequently involved by COVID-19. In addition, for lung collapse, the left lung (Group A: left lung 4.95%/right lung 4.65%, Group B: left lung 3.65%/right lung 3.15%) was also more severely affected than the right lung. There were significant differences between Groups A and B in the percentage of CT involvement of each lung region ($p < 0.05$), except for the total lung involved in inflation ($p = 0.152$). There were significant differences between Groups A and B in the percentage of CT involvement of each lung region ($p < 0.05$), except for the total lung involved in inflation ($p = 0.152$). In Group A, the median percentage of collapsed left lung was 20.00 (14.00–30.00), 18.50 (13.00–30.25) for the right lung and 19.00 (13.00–30.00) for the total lung. In contrast, the median percentage of collapsed left lung in Group B was 13.00

(10.00–14.75), 11.50 (10.00–15.00) for the right lung and 12.50 (10.00–15.00) for the total lung (Table 2).

In univariate analysis, almost all factors except cough, dyspnea, myalgia and total affected lung inflation could influence %LAA-950 emphysema. In multivariable analysis, patients with COVID-19 who had a higher left lung affected were most likely to have greater than 10% %LAA-950 emphysema (odds ratio 1.28, 95% CI 0.01–10.27; $p = 0.039$) (details in Table 3).

3.3 | CT image comparison

Axial chest CT scans of 44-year-old women from Group A and 44-year-old women from Group B were processed by 3D slice software and compared side by side (Figure 3).

4 | DISCUSSION

In our study, 66 patients with laboratory-confirmed COVID-19 pneumonia were evaluated. All 66 patients were admitted to the Renmin Hospital, Hubei University of Medicine, China from

Segment	Lung	A (%)	B (%)	p Value
Inflated affected	Total	77.00 (69.25–84.00)	73.00 (72.00–74.00)	0.152
	Left	81.00 (70.00–86.00)	88.00 (83.50–90.75)	<0.001
	Right	81.50 (69.75–87.00)	88.50 (85.00–90.00)	<0.001
Emphysema	Total	1.05 (0.30–2.85)	13.85 (10.43–17.90)	<0.001
	Left	1.30 (0.40–3.73)	14.00 (11.53–18.73)	<0.001
	Right	0.85 (0.20–2.50)	13.75 (10.18–16.83)	<0.001
Infiltrated	Total	14.65 (9.53–22.40)	8.75 (7.10–11.35)	0.001
	Left	14.55 (9.93–22.50)	9.40 (6.80–11.15)	0.001
	Right	13.95 (9.30–22.33)	8.40 (7.33–11.48)	0.003
Collapsed	Total	4.75 (4.10–7.10)	3.45 (2.93–3.93)	<0.001
	Left	4.95 (4.18–6.93)	3.65 (2.95–4.00)	<0.001
	Right	4.65 (3.88–6.75)	3.15 (2.83–3.78)	<0.001
Affected	Total	19.00 (13.00–30.00)	12.50 (10.00–15.00)	0.001
	Left	20.00 (14.00–30.00)	13.00 (10.00–14.75)	0.001
	Right	18.50 (13.00–30.25)	11.50 (10.00–15.00)	0.001

TABLE 2 Comparison of the percentage of involvement of each lung zone between the two groups

Note: Median of the percentage, the confidence interval for the median.

Variable		Univariate analysis OR	95% CI	p Value	Multivariate analysis OR	95% CI	p Value
Cough		0.92	0.24–3.46	0.901	-	-	-
Dyspnea		1.17	0.27–5.00	0.841	-	-	-
Myalgia		1.14	0.12–11.18	0.912	-	-	-
Inflated affected	Total	1.00	0.95–1.05	0.841	-	-	-
	Left	1.38	1.08–1.77	0.010	1.14	0.52–2.51	0.744
	Right	1.32	1.05–1.65	0.015	1.24	0.08–18.27	0.878
Infiltrated	Total	0.75	0.58–0.97	0.025	-	-	0.455
	Left	0.73	0.56–0.96	0.022	-	-	0.505
	Right	0.79	0.63–0.98	0.029	-	-	0.508
Collapsed	Total	0.05	0.01–0.33	0.002	-	-	0.706
	Left	0.06	0.01–0.38	0.003	8.02	-	0.879
	Right	0.08	0.02–0.38	0.002	0.47	-	0.947
Affected	Total	0.76	0.60–0.96	0.019	16.9	-	0.088
	Left	0.71	0.54–0.93	0.014	1.28	0.01–10.27	**0.039**
	Right	0.78	0.63–0.96	0.018	0.61	0.02–25.11	0.797

TABLE 3 Univariable and multivariable analysis and their associations

Note: Bold value indicate statistical significance $p < 0.05$.

February 2, 2020 to April 25, 2020. Patients were divided into two groups based on a threshold of %LAA-950 emphysema of 10%. Through Castaldi's report, we know that as %LAA-950 emphysema increases, so do individuals with severe centrilobular, PL, and PB types. The Lung CT Analyzer of the 3D Slicer was used to assess the percentage of involvement of each lung region between the two groups.

Our findings indicated that common clinical symptoms, such as cough, dyspnea, and myalgia, affected both groups of patients. Based on an in-depth analysis of the percentage of patients involved in each
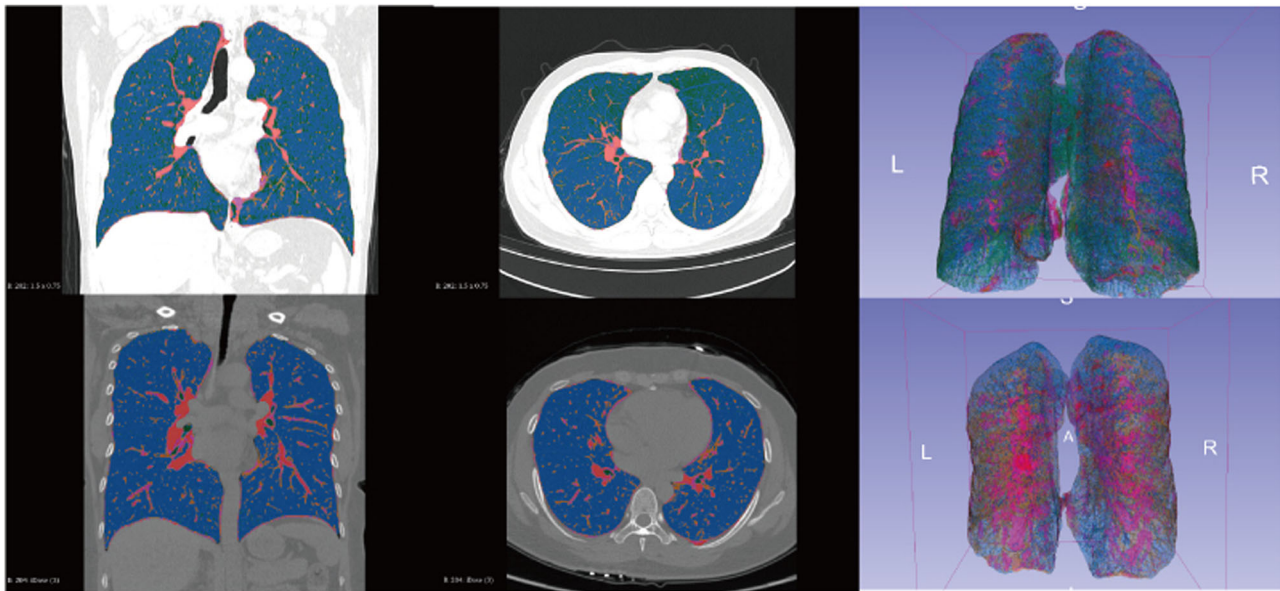
FIGURE 3 Forty-four-year-old women from Group A and 44-year-old women from Group B were processed by 3D slice software and compared side by side

lung zone in both groups, we found that the left lung was the most frequently involved site in COVID-19. Particularly, left lung collapse was more severe than the right lung collapse in both Group A and Group B. Additionally, inflated affected left lung and right lung, emphysema left lung and right lung and total lung, infiltrated left lung and right lung and total lung, collapsed left lung and right lung and total lung, affected left lung and right lung and total lung all differed significantly between the two groups. Using univariate and multivariate analysis, it was then concluded that a greater proportion of the left lung was affected in COVID-19 patients, most likely resulting in %LAA-950 emphysema greater than 10%.

In this study, we used the Lung CT Analyzer to identify five regions of interest. Patients were classified by one of these indicators, namely %LAA-950 emphysema. We have confirmed that there are significant differences between the two groups in the other four regions, even down to the exact location of the lungs. Although there have been a number of studies on the relationship between lung CT and the clinical features of patients with COVID-19,[27–29] few studies have begun by grouping patients appropriately. It is now important to recognize which patients may be serious and which may have been neglected. This is particularly important in the judgment of the patients. People with lower lung emphysema may have more collapsed segments. The collapsed segments there are, the more likely they are to lead to more serious clinical feature. Certainly, RT-qPCR-based nucleic acid testing is always the most important reference standard for diagnosis. However, early CT examinations can also play an important role in helping to manage patients in the emergency department in the first instance.

We are all aware that recent studies have demonstrated that CT of the chest plays a very vital role when RT-qPCR results are false negative in patients with COVID-19.[30,31] It has also been reported that for COVID-19, CT has a sensitivity of 98%.[32] Additionally, according to the official diagnostic and therapeutic protocol of the Chinese National Health Council (6th edition), CT examinations can not only diagnose COVID-19, but also monitor disease progression and assess outcomes. In the past, we always focused on CT imaging features, such as ground glass opacities (GGO), crazy paving patterns, airway changes and reversed halo signs.[33–38] In this study, we used software to split CT imaging into several parts for comparison. It could shed light on possible mechanisms of lung injury in COVID-19 and also provide better identification and accurate diagnosis.

Nowadays, computer vision-based detection algorithms for the detection of COVID-19 patients still receive less attention. Our study was retrospective and, therefore, a prospective empirical study is needed to validate our view.[2,39–42]

Our study has the following limitations. First, due to the retrospective nature of the study design, selection bias may occur. In addition, a longer follow-up period, larger sample size and baseline CT examination would be required to describe the full population of COVID-19 patients.[43–45]

5 | CONCLUSION

Computer vision and artificial intelligence methods can extract features from radiological images, saving critical time for disease control and management. In COVID-19, this approach was ahead of pathogenicity testing in terms of time to diagnosis.[46] Based on our retrospective study, patients in COVID-19 can be divided into two groups of %LAA-950 emphysema less than or greater than 10%, with significant differences in patients between the groups. Patients with less than 10% may have more serial features. Attention also needs to be paid to the patient's left lung, as it was more affected. Moreover, the percentage of affected left lung was an independent predictor of

emphysema in COVID-19 patients. An AI approach to CT imaging can reshape workflow, minimize the need for patient interaction, assist in automating the diagnosis process and improve the practice of attending physicians and radiologists.

AUTHOR CONTRIBUTIONS

Yiping Yin established the theoretical formalism. Yulin Zou wrote the manuscript with the support of Jing Wang and Ke Han. Ke Han and Yiping Yin edited and revised the manuscript. All authors contributed significantly to the work reported, and their contributions included simultaneously all being involved in the conception, study design, execution, acquisition of data, analysis, and interpretation. Or in all these areas, participating in the drafting, revision or critical review of the article, reviewing the final version to be published, agreeing on the journal to which the article was submitted, and agreeing to take responsibility for all aspects of the work.

ACKNOWLEDGMENTS

CONFLICT OF INTEREST

The authors declare no conflict of interest.

DATA AVAILABILITY STATEMENT

The data that support the findings of this study are available on request from the corresponding author. The data are not publicly available due to privacy or ethical restrictions.

ORCID

Yulin Zou http://orcid.org/0000-0001-5747-3720

REFERENCES

1. Huang C, Wang Y, Li X, et al. Clinical features of patients infected with 2019 novel coronavirus in Wuhan, China. *Lancet*. 2020;395(10223):497-506. doi:10.1016/S0140-6736(20)30183-5
2. Guan W, Ni Z, Hu Y, et al. Clinical characteristics of coronavirus disease 2019 in China. *N Engl J Med*. 2020;382(18):1708-1720. doi:10.1056/NEJMoa2002032
3. Yang X, Yu Y, Xu J, et al. Clinical course and outcomes of critically ill patients with SARS-CoV-2 pneumonia in Wuhan, China: a single-centered, retrospective, observational study. *Lancet Respir Med*. 2020;8(5):475-481. doi:10.1016/S2213-2600(20)30079-5
4. Mehta P, McAuley DF, Brown M, Sanchez E, Tattersall RS, Manson JJ. COVID-19: consider cytokine storm syndromes and immunosuppression. *Lancet*. 2020;395(10229):1033-1034. doi:10.1016/S0140-6736(20)30628-0
5. Docherty AB, Harrison EM, Green CA, et al. Features of 20133 UK patients in hospital with covid-19 using the ISARIC WHO Clinical Characterisation Protocol: prospective observational cohort study. *BMJ*. 2020;369:m1985. doi:10.1136/bmj.m1985
6. Priyanka null, Choudhary OP, Singh I, Patra G. Aerosol transmission of SARS-CoV-2: the unresolved paradox. *Travel Med Infect Dis*. 2020;37:101869. doi:10.1016/j.tmaid.2020.101869
7. Li X, Zeng X, Liu B, Yu Y. COVID-19 infection presenting with CT halo sign. *J Cardiovasc Imaging*. 2020;2(1):e200026. doi:10.1148/ryct.2020200026
8. Hui DS, et al. Impact of severe acute respiratory syndrome (SARS) on pulmonary function, functional capacity and quality of life in a cohort of survivors. *Thorax*. 2005;60(5):401-409. doi:10.1136/thx.2004.030205
9. Das KM, Lee EY, Singh R, et al. Follow-up chest radiographic findings in patients with MERS-CoV after recovery. *Indian J Radiol Imaging*. 2017;27(3):342-349. doi:10.4103/ijri.IJRI_469_16
10. Xie L, Liu Y, Xiao Y, et al. Follow-up study on pulmonary function and lung radiographic changes in rehabilitating severe acute respiratory syndrome patients after discharge. *Chest*. 2005;127(6):2119-2124. doi:10.1378/chest.127.6.2119
11. Ng CK, Chan JWM, Kwan TL, et al. Six month radiological and physiological outcomes in severe acute respiratory syndrome (SARS) survivors. *Thorax*. 2004;59(10):889-891. doi:10.1136/thx.2004.023762
12. Huang Y, Tan C, Wu J, et al. Impact of coronavirus disease 2019 on pulmonary function in early convalescence phase. *Respir Res*. 2020;21(1):163. doi:10.1186/s12931-020-01429-6
13. Liu D, Zhang W, Pan F, et al. The pulmonary sequalae in discharged patients with COVID-19: a short-term observational study. *Respir Res*. 2020;21(1):125. doi:10.1186/s12931-020-01385-1
14. Ye Z, Zhang Y, Wang Y, Huang Z, Song B. Chest CT manifestations of new coronavirus disease 2019 (COVID-19): a pictorial review. *Eur Radiol*. 2020;30(8):4381-4389. doi:10.1007/s00330-020-06801-0
15. Hassan H, Ren Z, Zhao H, et al. Review and classification of AI-enabled COVID-19 CT imaging models based on computer vision tasks. *Comput Biol Med*. 2022;141:105123. doi:10.1016/j.compbiomed.2021.105123
16. Oulefki A, Agaian S, Trongtirakul T, Kassah Laouar A. Automatic COVID-19 lung infected region segmentation and measurement using CT-scans images. *Pattern Recogn*. 2021;114:107747. doi:10.1016/j.patcog.2020.107747
17. Zhou X. Automatic segmentation of multiple organs on 3D CT images by using deep learning approaches. *Adv Exp Med Biol*. 2020;1213:135-147. doi:10.1007/978-3-030-33128-3_9
18. Pereira RM, Bertolini D, Teixeira LO, Silla CN, Costa YMG. COVID-19 identification in chest X-ray images on flat and hierarchical classification scenarios. *Comput Methods Programs Biomed*. 2020;194:105532. doi:10.1016/j.cmpb.2020.105532
19. Wang Y, Zhang Y, Liu Y, et al. Does non-COVID-19 lung lesion help? Investigating transferability in COVID-19 CT image segmentation. *Comput Methods Programs Biomed*. 2021;202:106004. doi:10.1016/j.cmpb.2021.106004
20. Amyar A, Modzelewski R, Li H, Ruan S. Multi-task deep learning based CT imaging analysis for COVID-19 pneumonia: classification and segmentation. *Comput Biol Med*. 2020;126:104037. doi:10.1016/j.compbiomed.2020.104037
21. Khan AI, Shah JL, Bhat MM. CoroNet: a deep neural network for detection and diagnosis of COVID-19 from chest x-ray images. *Comput Methods Programs Biomed*. 2020;196:105581. doi:10.1016/j.cmpb.2020.105581
22. Chen H, Jiang Y, Loew M, Ko H. Unsupervised domain adaptation based COVID-19 CT infection segmentation network. *Appl Intell*. 2022;52(6):6340-6353. doi:10.1007/s10489-021-02691-x
23. Hochreiter S, Schmidhuber J. Long short-term memory. *Neural Comput*. 1997;9(8):1735-1780. doi:10.1162/neco.1997.9.8.1735
24. Wang Y, Yang Q, Tian L, Zhou X, Rekik I, Huang H. HFCF-Net: a hybrid-feature cross fusion network for COVID-19 lesion segmentation from CT volumetric images. *Med Phys*. 2022;49(6):3797-3815. doi:10.1002/mp.15600
25. Ai T, Yang Z, Hou H, et al. Correlation of chest CT and RT-PCR testing for coronavirus disease 2019 (COVID-19) in China: a report

of 1014 cases. *Radiology*. 2020;296(2):E32-E40. doi:10.1148/radiol.2020200642

26. Castaldi PJ, San José Estépar R, Mendoza CS, et al. Distinct quantitative computed tomography emphysema patterns are associated with physiology and function in smokers. *Am J Respir Crit Care Med*. 2013;188(9):1083-1090. doi:10.1164/rccm.201305-0873OC

27. Wang Y, Dong C, Hu Y, et al. Temporal changes of CT findings in 90 patients with COVID-19 pneumonia: a longitudinal study. *Radiology*. 2020;296(2):E55-E64. doi:10.1148/radiol.2020200843

28. Zhou S, Wang Y, Zhu T, Xia L. CT features of coronavirus disease 2019 (COVID-19) pneumonia in 62 patients in Wuhan, China. *Am J Roentgenol*. 2020;214(6):1287-1294. doi:10.2214/AJR.20.22975

29. Ooi GC, Khong PL, Müller NL, et al. Severe acute respiratory syndrome: temporal lung changes at thin-section CT in 30 patients. *Radiology*. 2004;230(3):836-844. doi:10.1148/radiol.2303030853

30. Xie X, Zhong Z, Zhao W, Zheng C, Wang F, Liu J. Chest CT for typical coronavirus disease 2019 (COVID-19) pneumonia: relationship to negative RT-PCR testing. *Radiology*. 2020;296(2):E41-E45. doi:10.1148/radiol.2020200343

31. Huang P, Liu T, Huang L, et al. Use of chest CT in combination with negative RT-PCR assay for the 2019 novel coronavirus but high clinical suspicion. *Radiology*. 2020;295(1):22-23. doi:10.1148/radiol.2020200330

32. Fang Y, Zhang H, Xie J, et al. Sensitivity of chest CT for COVID-19: comparison to RT-PCR. *Radiology*. 2020;296(2):E115-E117. doi:10.1148/radiol.2020200432

33. Wang D, Hu B, Hu C, et al. Clinical characteristics of 138 hospitalized patients with 2019 novel coronavirus-infected pneumonia in Wuhan, China. *JAMA*. 2020;323(11):1061-1069. doi:10.1001/jama.2020.1585

34. Chung M, Bernheim A, Mei X, et al. CT imaging features of 2019 novel coronavirus (2019-nCoV). *Radiology*. 2020;295(1):202-207. doi:10.1148/radiol.2020200230

35. Fang Y, Zhang H, Xu Y, Xie J, Pang P, Ji W. CT manifestations of two cases of 2019 novel coronavirus (2019-nCoV) pneumonia. *Radiology*. 2020;295(1). doi:10.1148/radiol.2020200280

36. Qian L, Yu J, Shi H. Severe acute respiratory disease in a huanan seafood market worker: images of an early casualty. *Radiol Cardiothorac Imaging*. 2020;2(1):e200033. doi:10.1148/ryct.2020200033

37. Bernheim A, Mei X, Huang M, et al. Chest CT findings in coronavirus disease-19 (COVID-19): relationship to duration of infection. *Radiology*. 2020;295(3):200463. doi:10.1148/radiol.2020200463

38. Kay FU, Abbara S. The many faces of COVID-19: spectrum of imaging manifestations. *Radiol Cardiothorac Imaging*. 2020;2(1):e200037. doi:10.1148/ryct.2020200037

39. Ng MY, Lee EYP, Yang J, et al. Imaging profile of the COVID-19 infection: radiologic findings and literature review. *Radiol Cardiothorac Imaging*. 2020;2(1):e200034. doi:10.1148/ryct.2020200034

40. Li K, Wu J, Wu F, et al. The clinical and chest CT features associated with severe and critical COVID-19 pneumonia. *Invest Radiol*. 2020;55(6):327-331. doi:10.1097/RLI.0000000000000672

41. Chen N, Zhou M, Dong X, et al. Epidemiological and clinical characteristics of 99 cases of 2019 novel coronavirus pneumonia in Wuhan, China: a descriptive study. *Lancet*. 2020;395(10223):507-513. doi:10.1016/S0140-6736(20)30211-7

42. Kanne JP, Little BP, Chung JH, Elicker BM, Ketai LH. Essentials for radiologists on COVID-19: an update. *Radiology*. 2020;296(2):E113-E114. doi:10.1148/radiol.2020200527

43. Xu R, Du M, Li L, Zhen Z, Wang H, Hu X. CT imaging of one extended family cluster of corona virus disease 2019 (COVID-19) including adolescent patients and "silent infection". *Quant Imaging Med Surg*. 2020;10(3):800-804. doi:10.21037/qims.2020.02.13

44. Shah FM, Joy SKS, Ahmed F, et al. A comprehensive survey of COVID-19 detection using medical images. *SN Comput Sci*. 2021;2(6):434. doi:10.1007/s42979-021-00823-1

45. Loey M, Manogaran G, Khalifa NEM. A deep transfer learning model with classical data augmentation and CGAN to detect COVID-19 from chest CT radiography digital images. *Neural Comput Appl*. 2020;26:1-13. doi:10.1007/s00521-020-05437-x

46. Hassan H, Ren Z, Zhou C, et al. Supervised and weakly supervised deep learning models for COVID-19 CT diagnosis: a systematic review. *Comput Methods Programs Biomed*. 2022;218:106731. doi:10.1016/j.cmpb.2022.106731